JOURNAL OF MATERIALS SCIENCE **35** (2000) 3263 – 3268

Characterization of $\alpha \leftrightarrow \beta$ PbF_2 phase transition by several techniques

K. F. PORTELLA, K. R. RATTMANN, G. P. DE SOUZA,
C. M. GARCIA, M. P. CANTÃO
Laboratório Central de Pesquisa e Desenvolvimento-LAC Companhia Paranaense de Energia, Universidade Federal do Paraná, C. P. 19067, 81531-970, Curitiba, PR, Brazil

R. MUCCILLO
Instituto de Pesquisas Energéticas e Nucleares, Comissão Nacional de Energia Nuclear, C.P. 11049, Pinheiros, 05422-970, S. Paulo, SP, Brazil
E-mail: muccillo@usp.br

X-ray Diffraction (XRD), Dynamic-Mechanical Analysis (DMA), Impedance Spectroscopy (IS), and Scanning Electron Microscopy (SEM) have been used to the study of $\alpha \rightarrow \beta$ phase transition in PbF_2 pellets pressed uniaxially in the 37 MPa–480 MPa range. A mixture of β and α phases is detected and the α-phase content at room temperature is found to be dependent on the applied load. The dilation results on DMA, the phase identification by XRD, the ionic conductivity results by IS analysis and the SEM micrographs of β-PbF_2 pellets show evidences for the increase in α-phase content at the expense of the β-phase. SEM analysis provided further evidence for specimen sintering under heating at approximately 498 K. © *2000 Kluwer Academic Publishers*

---

1. Introduction

Two crystalline phases are known to occur in PbF_2 (lead fluoride): an orthorhombic α-phase with lattice parameters $a_0 = 3.899$ Å, $b_0 = 6.442$ Å and $c_0 = 7.651$ Å having a specific mass of 8.445 g/cm^3, and a cubic fluorite β-phase with lattice parameter $a_0 = 5.940$ Å and 7.750 g/cm^3 specific mass [1]. Lead fluoride is a solid electrolyte that exhibits a variety of interesting physical properties in both orthorhombic and cubic phases [2–8]. The $\alpha \rightarrow \beta$ phase transition occurs upon heating, with an endothermic variation in the 334 °C–344 °C temperature range. There is a volume variation of 10%, leading to crack formation in PbF_2 specimens heated at rates higher than 1 degree/min. At room temperature the β-phase is more stable than the α-phase [3]. The $\beta \rightarrow \alpha$ phase transformation can be achieved at pressures higher than 400 MPa [1]. At room temperature, the ionic conductivity of the β-phase is one order of magnitude higher than that of the α-phase. The charge carriers responsible for the ionic conduction are interstitial fluorine ions. Many studies have been carried out in lead fluoride due to its relatively high ionic conductivity (superionic conduction) at temperatures above 437 °C.

Specimens with different α/β ratio have been prepared by uniaxially pressing lead fluoride powders under different pressing loads to study the $\alpha \rightarrow \beta$ phase transformation by using several techniques: X-ray Diffraction (XRD), Dynamic-Mechanical Analysis (DMA), Impedance Spectroscopy (IS), and Scanning Electron Microscopy (SEM).

2. Experimental

Powders in the orthorhombic phase (α-PbF_2) have been prepared using p.a. grade reagents; powders in the cubic phase (β-PbF_2) have been prepared by heating α-PbF_2 at about 633 K, a temperature higher than its phase transition temperature (607 K–617 K). The powders have been pressed to 13 mm diameter pellets under vacuum in a Perkin-Elmer die at different pressures (in MPa): 37, 74, 148, 222, 297, 334, 371, 408 and 480. Pellets pressed to 297 MPa have been analyzed before and after annealing at 533 K, and after heating to 633 K for β-PbF_2 formation.

X-ray diffraction of specimens were measured using a Philips (X'Pert MPD) diffractometer with CuK_α radiation operating at 40 kV and 50 mA. The diffraction patterns were used to identify the structural phases of the specimens.

Impedance spectroscopy measurements of both α- and β-PbF_2 were carried out in pellets prepared by uniaxially pressing in the 37 to 480 MPa range. Measuring cells of the Pt $|x$-$PbF_2|$ Pt type ($x = \alpha, \beta$ or $\alpha + \beta$, Pt = sputtered platinum) were set up inside a tubular furnace. The electrical measurements were performed in the 10 mHz–1 MHz frequency range with a 5 mV signal amplitude at 298 K and 423 K in air with an electrochemical impedance analyzer (Solartron 1255 with a EG&G PAR 283 potenciostat/galvanostat) connected to a computer. The impedance spectroscopy data were plotted as $[-Z'' \times Z']$ diagrams (Nyquist diagrams) and $[\log |Z| \times \log f]$ (Bode diagrams). Z'' and Z' stand for the imaginary and the real components of the electrical impedance, respectively; $|Z|$ is the modulus of the impedance and f the frequency of the applied voltage signal. The total resistivity of the specimen is taken at the intercept of the impedance response with the real axis in the low frequency region of the impedance diagram [9].

For Dynamic-Mechanical Analysis, the sinusoidal deflection of the specimens (after applying a sinusoidal oscillating force) was measured as a function of temperature with a model 242 Netzsch Dynamic-Mechanical Analyzer operating in the following conditions: compression mode at 5 Hz; 294 K–633 K temperature range; 1.0 K/min heating rate; 50 mL/min nitrogen flow rate. Dynamic-mechanical analysis has already been used to the study of polymeric and composite materials, mainly to verify relationships between dynamical properties and structural parameters, as for example the degree of crystallinity and molecular orientation as a function of environmental or external variables as temperature, pressure, signal frequency, etc. [10].

The analysis of polished and fractured pellet surfaces has been done in specimens thermally treated at temperatures below and above the $\alpha \rightarrow \beta$ transition temperature, using a model XL30 Philips Scanning Electron Microscope. Gold was applied to the pellet surfaces by sputtering.

3. Results and discussion

Fig. 1a and b show XRD patterns of PbF_2 as obtained (α-phase) and after transition to β-PbF_2, respectively. These results are in good agreement with the JCPDS data for these compounds. No impurities have been detected.

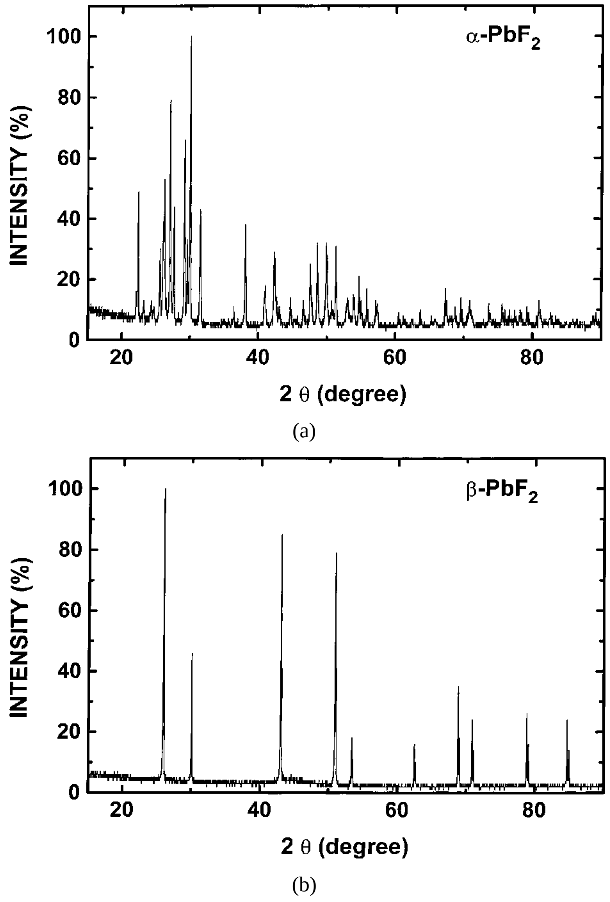

(a)

(b)

Figure 1 XRD patterns of α-PbF_2 (a) and β-PbF_2 (b).

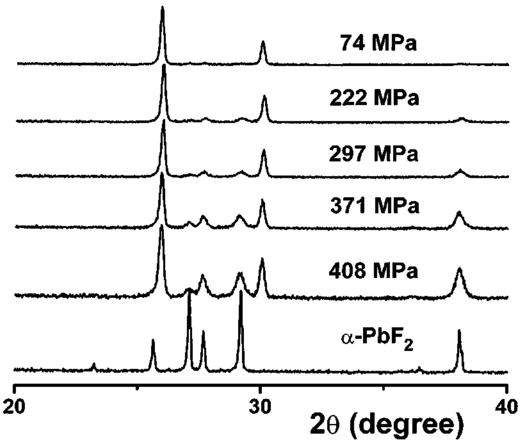

Figure 2 XRD patterns of β-PbF_2 pellets pressed at different loads: 74 MPa, 222 MPa, 297 MPa, 371 MPa, 408 MPa; pattern at the bottom: α-PbF_2 as prepared.

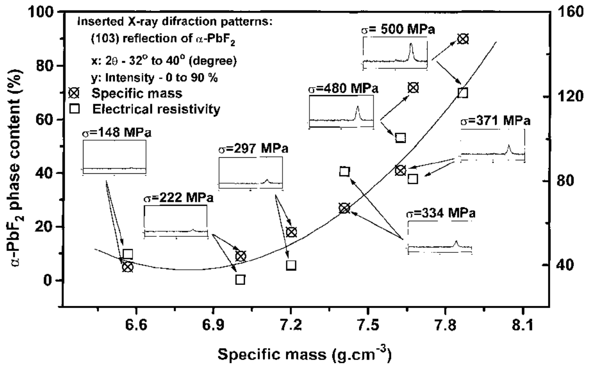

Figure 3 α-PbF_2 phase content and electrical resistivity at 298 K as a function of specific mass of β-PbF_2 pellets pressed at different loads: 148 MPa, 222 MPa, 297 MPa, 334 MPa, 371 MPa, 408 MPa, 480 MPa and ~500 MPa. XRD patterns of the (103) reflection α-PbF_2 are shown as a function of the load.

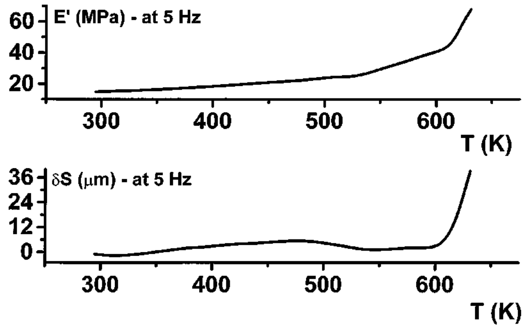

Figure 4 Room temperature to 633 K Dynamic-Mechanical Analysis of β-PbF_2 pressed at 297 MPa.

Fig. 2 shows XRD patterns of β-PbF_2 pellets after pressing from 74 MPa to 408 MPa in the 2θ range where the most prominent X-ray reflections occur. An increase of the α-PbF_2 content at the expense of the β-PbF_2 phase is detected. The α-PbF_2 content in the lead fluoride pellet is larger than that previously reported for pellets prepared under higher pressures [3], but close to the values reported for pellets obtained by pressing at 400 MPa [2]. The XRD patterns of pellets prepared by pressing powders up to 400 MPa show a mixture of both α and β phases.

Electrical measurements carried out in pellets pressed under different loads allowed for the study of the $\alpha \rightarrow \beta$ phase transition. An increase of approximately one order of magnitude is measured on the total electrical resistivity of pellets prepared with higher pressure. Fig. 3 shows the electrical resistivity,

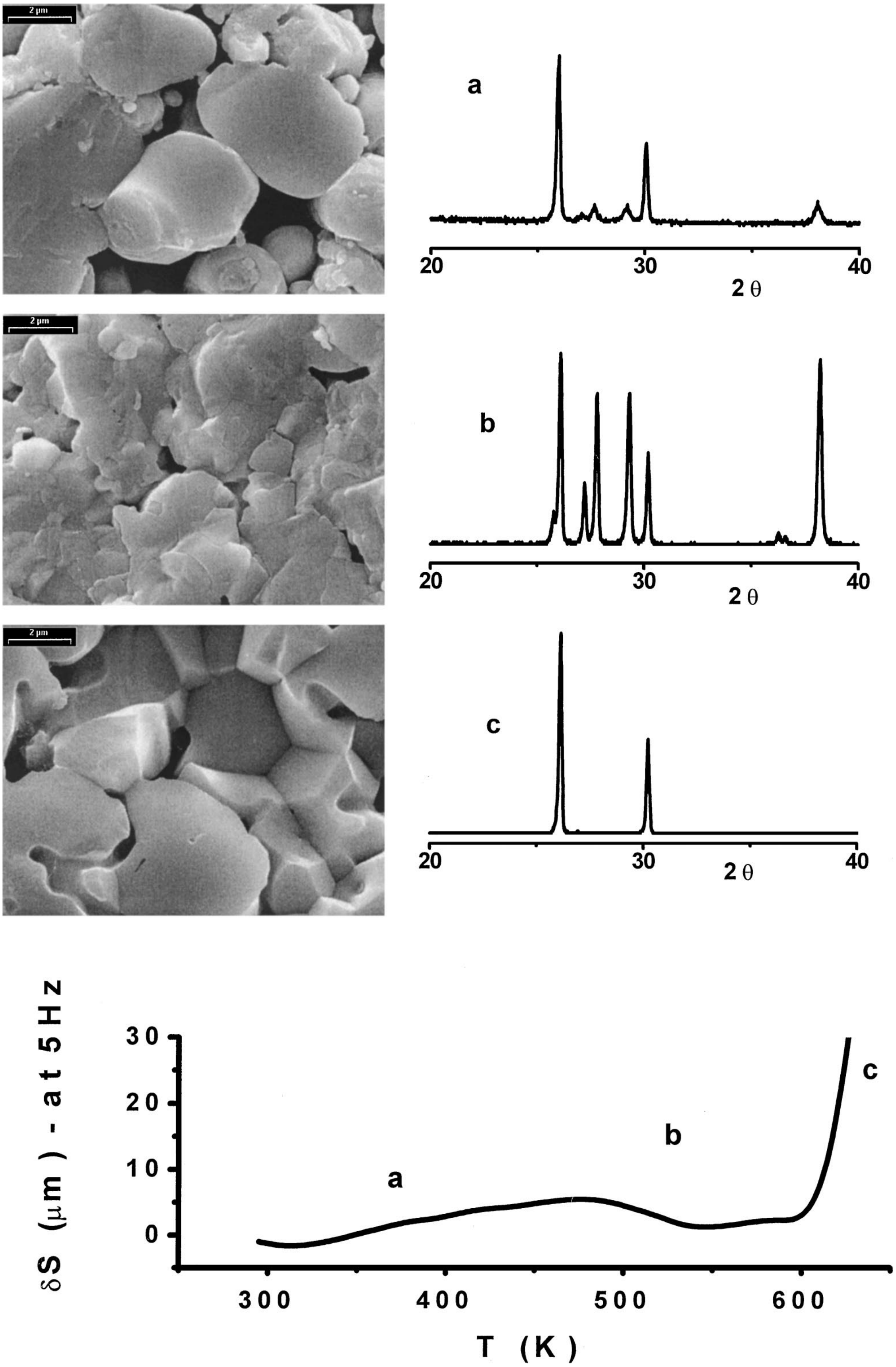

Figure 5 Bottom: Room temperature to 673 K Dynamic-Mechanical Analysis of β-PbF$_2$ pressed at 297 MPa; Top: SEM micrographs of fractured surfaces and room temperature XRD patterns of the as pressed pellet (a); after heating at 573 K (b); after heating to 633 K, cooling to room temperature and further heating to 573 K.

determined at 298 K as a function of the specific mass. In the same figure, the relative α-phase content, expressed by the area under the (103) reflection (the main X-ray diffraction peak of that phase), is also plotted as a function of the specific mass. Both the electrical resistivity and the α-PbF_2 phase content increase for increasing specific mass. The results are in good agreement with reported data [2].

In Fig. 4 results on Dynamic-Mechanical Analysis (Young's modulus E'—top figure, specimen dilation δS—bottom figure) from room temperature up to the phase transition temperature of a β-PbF_2 pellet pressed at 297 MPa are shown. The following main features can be drawn, specifically between 473 K and 633 K: a contraction of approximately 10% of the sample volume in the 473 K–534 K range, due to recovering of the α-PbF_2 phase; a non-variation of the volume in the 534 K–604 K range and complete recovering of the α-PbF_2 phase; and finally, a large sample volume variation in the 604 K–633 K range, due to the onset of the $\alpha \rightarrow \beta$ phase transition. To our knowledge, this is the first experimental evidence of phase transition in PbF_2 by dynamic-mechanical analysis.

These results are best understood when the dilation curves, the XRD patterns and the SEM micrographs are observed altogether, as shown in Fig. 5.

The XRD pattern of β-PbF_2 pellet after pressing at 297 MPa is shown in Fig. 5a. It presents a $\alpha + \beta$ mixture of PbF_2 (with about 10% α-phase) due to partial transformation after pressing. The corresponding SEM image of a fractured surface shows powder agglomerates and large interparticle pores. The analysis carried out at room temperature after thermal treatment up to 533 K is shown in Fig. 5b. Sintering of the specimen with pore shrinkage is evident in the SEM micrograph. Afterwards, analysis by XRD and SEM are performed at room temperature in a pellet cooled from 633 K, a temperature above the phase transition. The results are shown in Fig. 5c. The SEM micrograph shows that sintering has already started. Moreover, the α-PbF_2 content determined by X-ray diffraction increases and a phase transition occurs at 533 K according to the DMA dilation curve.

Samples prepared by heating up to 633 K (to promote $\alpha \rightarrow \beta$ phase transition) and cooled to room temperature were further heated to 573 K leading to densification. XRD patterns did not show α-PbF_2 phase in these pellets as in Fig. 5b. In Fig. 6, SEM images and XRD patterns of β-PbF_2 pellets pressed at lower pressures (37 MPa) and thermally treated at 573 K are shown. The XRD patterns show less α-phase than in not heated samples.

The results on Fig. 6 seem to indicate a pressure-induced increase in α-PbF_2 phase content. A reconstructive first-order transition during heating, involving a large number of crystalline defects, was reported by Samara for PbF_2 specimens pressed at 0.12 GPa, and also at 280 K for increasing pressures [1]. The micrographs in Fig. 6 show also pores on the fractured surfaces. These defects seem to have been produced by small crystals that grow on the surfaces, as shown in Fig. 7a. The quantity of these crystals is found to be

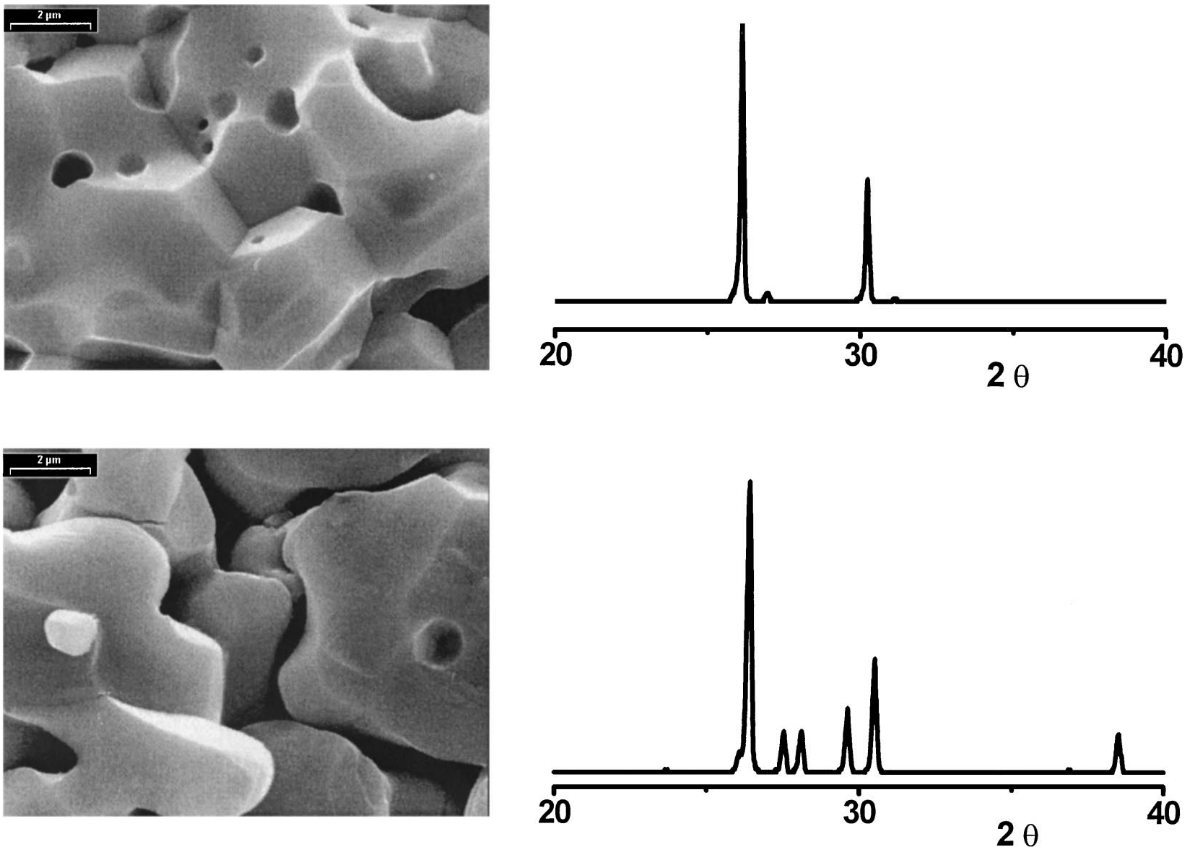

Figure 6 SEM micrographs of fractured surfaces and room temperature XRD patterns of the PbF_2 pellet: after heating to 673 K, cooling to room temperature and heating to 573 K (a); after pressing at 74 MPa and heating to 573 K (b).

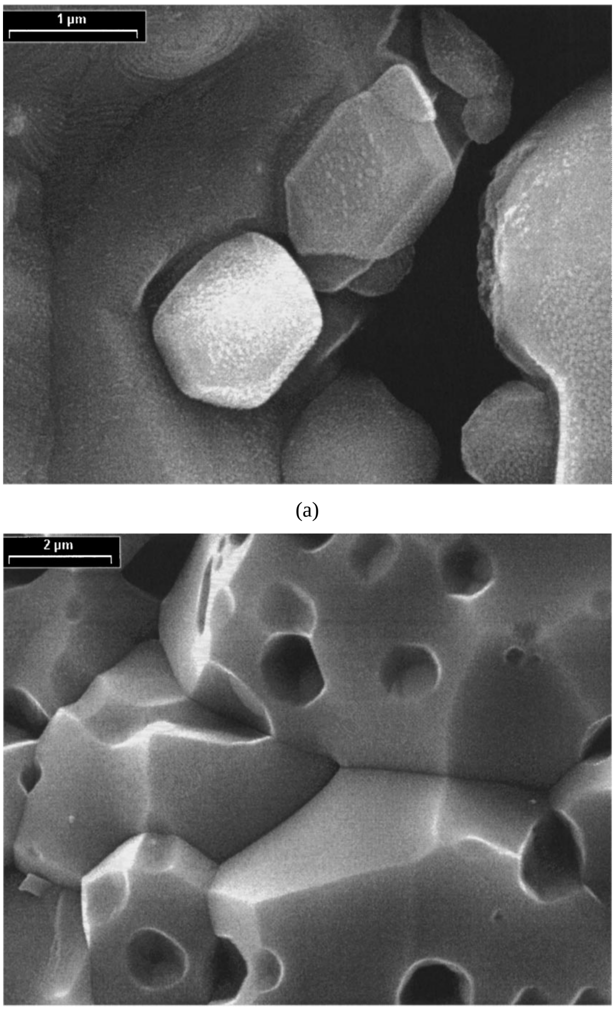

(a)

(b)

Figure 7 SEM micrographs of fractured surfaces of PbF_2 pellet: pressed at 74 MPa and heating to 533 K (a); after heating to 633 K the pellet pressed at 297 MPa.

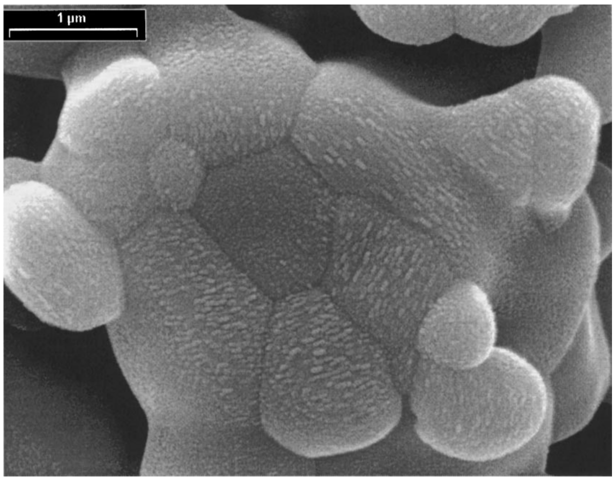

Figure 8 SEM micrograph of a fractured surface of PbF_2 pellet pressed at 74 MPa and heated to 533 K showing grains with oriented crystals.

proportional to the α-PbF_2 phase content in the pellets. After complete recovering of the β-PbF_2 phase, these crystals are not detected, but the defects on the β-PbF_2 surface still remain as shown in Fig. 7b.

Fig. 8 a SEM image of a fractured specimen is shown. Grains containing oriented crystals are clearly seen.

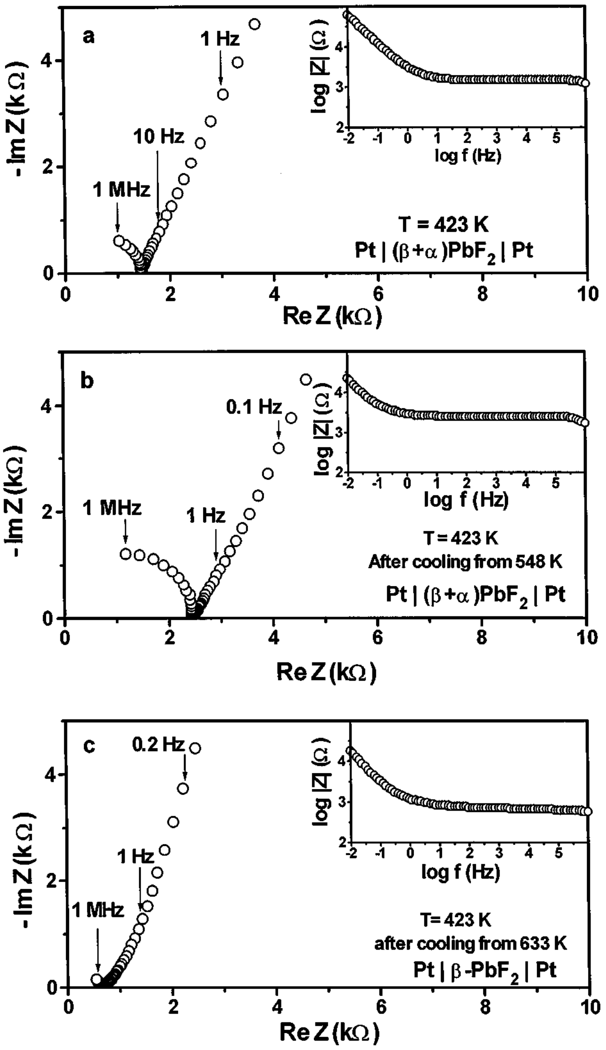

Figure 9 Impedance spectroscopy diagrams (Nyquist and Bode) of PbF_2 pellets measured at 423 K: after pressing (a); after heating to a temperature below the $\alpha \rightarrow \beta$ phase transition (548 K) and cooling to 423 K (b); and after heating to a temperature above the $\alpha \rightarrow \beta$ phase transition (633 K) and cooling to 423 K.

A detailed analysis of the impedance spectroscopy has been carried out [11] and will be published elsewhere [12]. Here will be reported some impedance spectroscopy results about the influence of thermal variations, and consequent phase transitions, on the electrical properties of β-PbF_2.

Fig. 9 shows three impedance spectroscopy (Nyquist) diagrams—and the corresponding Bode diagrams—of PbF_2 specimens after measurements at 423 K. These specimens, with 13 mm diameter and 1 mm thickness, were prepared by pressing the PbF_2 powders at 297 MPa, achieving a density of 7.11 g/cm^3. They contain approximately 10% of the alpha phase (Cf. Fig. 3). The values in Fig. 9a were taken just after heating the specimen up to the temperature of measurement, i.e., below the $\alpha \rightarrow \beta$ phase transition temperature (613 K). Fig. 9b shows the impedance diagram of the same specimen after heating up to 548 K—below the $\alpha \rightarrow \beta$ phase transition temperature—and cooling down to 423 K. The electrical resistivity of the specimen increases due to an increase in the α-phase content. The specimen is then heated up to 633 K, a temperature higher than the $\alpha \rightarrow \beta$ phase transition temperature and cooled down to 423 K. The results, indicating a decrease in the electrical resistivity of the specimen as a result of the β-phase formation, are shown in Fig. 9c. Only the β-phase is present, as shown in the X-ray diffraction pattern of Fig. 5c.

4. Conclusions

Lead fluoride specimens prepared by pressing powders under different loads have been studied by X-ray diffraction, dynamic-mechanical analysis, impedance spectroscopy and scanning electron microscopy. All results are explained on the basis of the alpha → beta phase transition, known to occur in this solid electrolyte at approximately 613 K. The dynamic-mechanical analysis of PbF_2, here reported for the first time, provides further evidence of that phase transition. Moreover, sintering of lead fluoride pressed pellets and formation of crystals in their internal surfaces were detected by scanning electron microscopy.

Acknowledgements

The authors acknowledge COPEL, IPEN, CNPq, RHAE, FINEP/PADCT, PRONEX and FAPESP for financial support, and Dr. E. N. S. Muccillo for critical comments.

References

1. D. A. JONES, *Proc. Royal Soc.* **65B** (1955) 165.
2. G. A. SAMARA, *J. Phys. Chem. Sol.* **40** (1979) 509.
3. J. H. KENNEDY, R. MILES and J. HUNTER, *J. Electrochem. Soc.* **120** (1973) 1441.
4. C. C. LIANG and A. V. JOSHI, *ibid.* **122** (1975) 466.
5. J. H. KENNEDY and R. C. MILES, *ibid.* **123** (1976) 47.
6. R. W. BONNE and J. SCHOONMAN, *ibid.* **124** (1977) 28.
7. *Idem. ibid.* **125** (1978) 1628.
8. J. SCHOONMAN, K. E. D. WAPENAAR, G. OVERSLUIZEN and G. J. DIRKSEN, *ibid.* **126** (1979) 709.
9. "Impedance Spectroscopy—Emphasizing Solid Materials and Systems," edited by J. R. Mc. Donald (Wiley Interscience, New York, 1987).
10. T. MURAYAMA, "Dynamic-Mechanical Analysis of Polymeric Materials" (Elsevier, The Netherlands, 1978).
11. K. F. PORTELLA, Doctorate Thesis, IPEN, Universidade de S. Paulo, Brazil (1997) in Portuguese.
12. K. F. PORTELLA, C. M. GARCIA, G. P. DE SOUZA and R. MUCCILLO, to be published.

Received 27 May
and accepted 21 December 1999